NJC

ROYAL SOCIETY OF CHEMISTRY

PAPER

View Article Online
View Journal | View Issue



Cite this: *New J. Chem.*, 2025, 49, 514

# Linear oligopeptide formation from alanine-diketopiperazine in acidic aqueous solutions using interfacial nano-pulsed discharge plasma†

Mitsuru Sasaki, *[abc] Kouki Nonaka,[d] Yuka Sakai,[d] Tetsuo Honma,[e] Tomohiro Furusato[f] and Kunio Kawamura*[g]

Received 9th December 2023,
Accepted 17th November 2024

DOI: 10.1039/d3nj05664c

rsc.li/njc

Traditionally, synthesis of peptides using solid- or liquid-phase methods requires organic solvents, which goes against the fundamentals of green chemistry. In our previous study, we successfully demonstrated a green synthesis process involving alanine oligopeptides from alanine–diketopiperazine (alanine–DKP) using pulsed discharge plasma. By optimizing the conditions for oligopeptide synthesis, we improved the green synthesis of alanine oligopeptides by performing plasma irradiation in an acidic aqueous solution. The yield of alanyl–alanyl–alanine from alanine–DKP is approximately 30% within 3–20 min. The addition of alanylalanine enhances the formation of higher oligopeptides. Furthermore, LC-MS analysis shows trace amounts of glycine–DKP, glycine oligopeptides, glutamic acid, pyruvic acid, and pyroglutamic acid, which implies the reaction mechanism for the spontaneous elongation of higher oligopeptides from alanine–DKP through the ring opening of alanine–DKP and the radical formation of amino acids. Thus, the formation of DKP is advantageous for the formation of oligopeptides and does not inhibit oligopeptide elongation. This study provides useful insights into the chemical evolution of oligopeptides and the development of environmentally friendly oligopeptide formation processes.



## Introduction

Peptides are important for both fundamental and practical applications. The roles of peptides in organisms and their applications in different fields have been frequently summarized in the literature,[1,2] and their applications include the synthesis of peptide medicines[3,4] and the development of biosensors.[5,6] Peptides are conventionally fabricated using solid- or liquid-phase methods involving a series of synthetic processes.[7,8] However, a multistep synthesis using organic solvents and protecting groups, such as 9-fluorenylmethyloxycarbonyl (FMOC) and *tert*-butoxycarbonyl (BOC), is not regarded as suitable for green chemistry. However, alternative pathways have not yet been identified.

The formation of peptides in aqueous solutions has been extensively studied from the perspective of the chemical evolution of proteins on Hadean Earth.[9–12] According to the studies of peptide formation in aqueous phases in relation to the origin-of-life problem, simulation experiments of a hydrothermal vent system in the deep ocean have shown that oligopeptides are formed from monomeric amino acids.[11,12] However, the efficiency of such processes is not high, typically approximately 0.1%; hence, alternative pathways have been proposed to improve the efficiency of the formation of higher oligopeptides. This low efficiency can be attributed to two reasons. First, diketopiperazine (DKP) formation stops the elongation of higher oligopeptides. We have developed successful methods to prevent DKP-induced termination, including the use of a tetrapeptide and a specific combination of amino acids, such as glutamic and aspartic acids.[12,13] Second, the formation of amide bonds causes dehydration, which makes the formation of peptides in an aqueous medium disadvantageous from a thermodynamic viewpoint. However, energy-supply methods have not been sufficiently investigated.

[a] *Institute of Industrial Nanomaterials, Kumamoto University, 2-39-1 Kurokami, Chuo-ku, Kumamoto 860-8555, Japan*
[b] *Faculty of Advanced Science and Technology, Kumamoto University, 2-39-1 Kurokami, Chuo-ku, Kumamoto 860-8555, Japan*
[c] *International Research Organization for Advanced Science and Technology, Kumamoto University, 2-39-1 Kurokami, Chuo-ku, Kumamoto 860-8555, Japan*
[d] *Graduate School of Science and Technology, Kumamoto University, 2-39-1 Kurokami, Chuo-ku, Kumamoto 860-8555, Japan*
[e] *Department of Industrial Systems Engineering, National Institute of Technology, Hachinohe College, 16-1 Uwanotai, Tamonoki, Hachinohe, Aomori 039-1192, Japan*
[f] *Graduate School of Engineering, Nagasaki University, 1-14 Bunkyo-machi, Nagasaki 852-8521, Japan*
[g] *The Faculty of Human Environmental Studies, Hiroshima Shudo University, 1-1-1 Ozuka-higashi, Asaminami-ku, Hiroshima 731-3195, Japan*

† Electronic supplementary information (ESI) available. See DOI: https://doi.org/10.1039/d3nj05664c

 

The use of discharged plasma for chemical reactions and treatments has been extensively studied for use in green technology.[14–18] Examples include the degradation of toxic compounds and the synthesis of carbon nanoparticles. The energy range produced by the discharged plasma is relatively high. Thus, plasma discharge treatment has frequently been adopted for the degradation of waste chemicals. In general, thermal plasmas are strong, whereas nonthermal plasmas are relatively weak.[19,20] Therefore, thermal plasma is not considered suitable for organic synthesis in aqueous solutions.

We attempted to use electric discharge pulse plasma as an energy source to form amide bonds between amino acids. In addition, we examined whether DKP can be used as a starting material for the formation of higher oligopeptides as it generally inhibits the elongation of oligopeptides, even in processes using solid- and liquid-phase synthesis methods. In our previous study, we discovered that oligopeptide elongation from DKP was possible by irradiation with nano-pulsed discharge plasma.[21] Surprisingly, thermal plasma was more efficient than nonthermal plasma for this reaction. This pathway possesses strong potential as a technological seed for the environmentally harmless synthesis of oligopeptides without the use of organic solvents or protection groups, even those that are normally synthesized by pure organic chemistry.

In this study, we studied the scope of this fundamental reaction for the efficient formation of oligopeptides. We determined that the formation of alanine tri- and tetra-oligopeptides proceeded more efficiently under strongly acidic conditions. In addition, we investigated the conditions required for the elongation of higher oligopeptides and discussed the reaction mechanism of higher oligopeptide formation.

## Experimental

### Nano-pulsed discharge plasma setup

The experimental setup for the generation of the pulsed discharge plasma was based on our previous method.[21] A schematic representation of the experimental setup and its photo is provided in Fig. S1 in the ESI.† Sample solutions (10 mL) containing 100 mM DKP and alanine (**Ala-DKP**) were prepared at different initial pH values. The solutions (pH 4.7) were prepared without the addition of an acid to the 100 mM **Ala-DKP** solution, and the solutions at pH 1.7 and 1.0 were prepared with nitric acid. A 10 mL sample solution was added to a reactor (80 mL glass vessel), which was partially isolated from the atmosphere by a silicon rubber stopper. Then, the discharge plasma was generated using a pulsed power supply (MPC3000S-25LP, Suematsu Electronics Manufacturing Co. Ltd) through a tungsten anode (outer diameter: 1.0 mm, NILACO Co. Ltd) to a stainless-steel cathode (outer diameter: 1.59 mm), which was adjusted to 2 mm for the thermal plasma. The pulse frequency and width were 50–250 pps (pulse per s) and 0.1 μs, respectively. The pulse voltage and current were approximately 14–25 kV and 135–145 A at pH 4.7 and 8–9 kV and 170–180 A at pH 1.0, respectively. Discharge was conducted at 50, 100, 200, and 250 pps for up to 20 min at atmospheric pressure without controlling the temperature of the reactor, unless noted otherwise.

### Sample analysis

The pH was measured using a portable pH meter (LAQUA, HORIBA Co. Ltd, Japan). Inorganic ions were analyzed using an ion chromatograph IA-300 (TOA DKK Co. Ltd, Japan) with an ion-exchange column PCI-211 and a guard column PCI-211G (TOA DKK Co. Ltd, Japan). The eluent was provided by TOA DKK for the PCI-211 column and separation was performed at 1.1 mL $min^{-1}$ with a calibration mixture IA-AS1 (TOA DKK Co. Ltd, Japan).

The amount of alanine was analyzed by gas chromatography with a flame ionization detector (GC-FID) using a gas chromatograph (Shimadzu GC-2010 Plus, Shimadzu Co. Ltd, Japan) and an SH-Rxi-PAH detector (length: 30 m and inner diameter: 0.25 mm). The gradient was performed as follows: the column was heated from room temperature to 100 °C for 0.5 min before being further heated to 275 °C for 4 min at a gradient rate of 30 °C $min^{-1}$ using He as the carrier gas. A sample volume of 1 mL was injected at 250 °C and 115 kPa into the column.

The Ala oligopeptides in the reaction products were analyzed *via* high-performance liquid chromatography (HPLC) using a JASCO system with an MD-4017 photodiode array detector (JASCO Co. Ltd, Japan). The linear gradient on a reversed-phase column Inertsil™ ODS-3V (mean particle size: 3 μm, inner diameter: 4.6 mm, and length: 250 mm; GL Science, Japan) was applied using a mixture of an eluent containing 5 mM phosphate and 3.6 mM 1-hexanesulfonic acid with methanol from 1% (0 min), 10% (16 min), and 10% (25 min) at 35 °C.

LC-MS analysis was performed using an ultra performance liquid chromatography (UPLC) system (Waters UPLC PDA detector) on an Inertsil Amide column. The separation of UPLC was performed with a mixture of 63% water, 7% of aqueous solution of 1% formic acid, and 30% methanol at 0.3 mL $min^{-1}$. Mass spectrometry (MS) analyses were conducted using an electrospray ionization (ESI) detector at 2 kV negative or 2.5 kV positive at a source temperature of 150 °C. An MS scan was performed in the range of 50–1200 Da at a step rate of approximately 0.01 Da.

### Current and voltage measurements

Current–voltage measurements were performed using an oscilloscope DL9140L (Yokogawa Test & Measurement Co. Ltd, Japan) equipped with a Rogowski coil 110A (Pearson Electronics, USA). The current was measured by reducing it to 1/10 using a BNC-type fixed attenuator (BA-PJ-20, TO-CONNE Co. Ltd, Japan), and the voltage was measured using a high-voltage probe P6015A (Tektronix Inc., USA).

## Results and discussion

### Reaction behavior of Ala-DKP at an initial pH of 4.6

The reaction behavior of **Ala-DKP** was investigated at an initial pH of 4.6 using a new power supply, which is the successor

model of MPC3000C used in our previous study.[21] The reaction behavior at different irradiation times of 3–30 min (Fig. 1) was comparable to that obtained using the old power supply. The products at pH 4.6 without the addition of a pH buffering agent were similar to those determined in our previous study. This indicated that the formation of higher oligopeptides from **Ala-DKP** was reproducible under different experimental and instrumental conditions. In general, the generation of plasma is often sensitive and dependent on several conditions, such as the distance between the interface and electrode and humidity around the interface. Therefore, the reproduction between the present and previous studies shows the usefulness of the present reaction technique.

However, the formation of **Ala-Ala-Ala** was less frequently observed in the present study than in the previous study. In addition, the number of unknown products increased with increasing discharge times and corresponded to the difference between the initial amount of **Ala-DKP** and the total amount of Ala, **Ala-Ala**, **Ala-Ala-Ala**, and **Ala-Ala-Ala-Ala**, and the remaining **Ala-DKP**.

The influence of the discharge frequency was inspected under the condition that the total number of discharge shots was maintained at 60 000 shots. Thus, the frequency was varied at 50, 100, 200, and 250 pps and the irradiation periods were reduced to 20, 10, 5, and 4 min, respectively (Fig. 1b). The production behavior of **Ala-Ala**, **Ala-Ala-Ala**, and **Ala-Ala-Ala-Ala** was not notably dependent on the frequency, whereas a small amount of **Ala-Ala-Ala** was detected during the experiment at frequencies of 100–250 pps. The detection of **Ala-Ala-Ala** was probably caused by the degradation of **Ala-Ala-Ala-Ala** to **Ala-Ala-Ala** due to the high irradiation frequency. In addition, the net conversion ratio, including unknown products at frequencies of 100–250 pps at an irradiation time of 4–10 min, was considerably higher than that at 50 pps at 20 min because the unknown products were detected at frequencies of 100–250 pps.

## Nitric acid formation by nano-pulsed discharge plasma

In our preliminary study, we determined that thermal plasma was suitable for the synthesis of higher oligopeptides from DKP, whereas nonthermal plasma was inefficient. The results of the present study are consistent with this assumption. In a previous study,[21] we used a starting mixture containing DKP without controlling the pH of the solution. During the experiments, we noticed that the strong light caused by the nano-pulsed discharge gradually disappeared after 10–20 min of plasma irradiation. Therefore, we assumed that the plasma environment might fit gradually into the chemical environment for the efficient formation of higher oligopeptides during the irradiation of nano-pulsed discharges.

Based on this assumption, we suspected that temperature and/or pH would affect oligopeptide formation.[15] Thus, we tested the temperature and pH profiles during the nano-pulsed discharge of the reaction mixture, which was initially controlled at pH 4.6. The temperature behavior was consistent with our previous study, where the temperature reached approximately 60 °C (Fig. S1a, ESI†). However, the pH value rapidly decreased at the initial stage and gradually reached a pH of 1.67 after an irradiation time of 30 min (Fig. S1b, ESI†). This result was consistent with the fact that the discharge plasma forms nitrogen oxide in the atmosphere.

We examined the amount of nitric acid in a sample solution exposed to the nano-pulsed discharge plasma for 20 min using ion chromatography. The inorganic ions analyzed using ion-exchange chromatography are summarized in Table 1. The generation of nitrate and nitrite indicates that these ions were formed from the nitrogen gas present in the atmosphere. The calculated pH value based on the amount of nitrate ions is 1.93, which is consistent with the experimentally measured pH of 1.95, where the amount of nitrite was omitted because of its weak acidity. The volume of nitrogen gas in the vessel that was converted to nitrate was calculated as 1.3 mL. This indicates that the pH of the aqueous solution was readily decreased by the discharge plasma. The formation of nitrate from nitrogen and oxygen gases by the discharge plasma is consistent with previous studies.[22–25]

## Reaction behavior of Ala-DKP at initial pHs of 1.7 and 1.0

In this section, we determined that the pH considerably decreased during irradiation with the nano-pulsed discharge plasma. Therefore, we examined the reaction products at different pH values (Fig. S2, ESI†). The yields of **Ala-Ala** and **Ala-Ala-Ala** significantly increased with decreasing pH values.

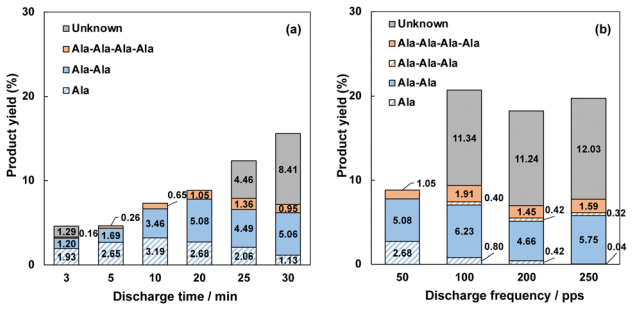


Fig. 1 Product yield from **Ala-DKP** at pH 4.6. (a) Influence of the discharge time and the (b) discharge frequency on the product yield. [**Ala-DKP**] = 100 mM (10 mL), initial pH: 4.6, discharge frequency: 50–250 pps, and discharge time: 3–30 min.

Table 1 Amount of inorganic ions after irradiation with nano-pulsed discharge plasma

| Ions | Amount/mg $L^{-1}$ |
|---|---|
| $PO_4^{3-}$ | 0.00 |
| $F^-$ | 0.00 |
| $Cl^-$ | 0.13 |
| $NO_2^-$ | 202 |
| $Br^-$ | 0.00 |
| $NO_3^-$ | 726 |
| $SO_4^{2-}$ | 0.00 |

[**Ala-DKP**] = 100 mM (10 mL), initial pH: 4.6, discharge frequency: 50 pps, and irradiation time: 20 min.

 

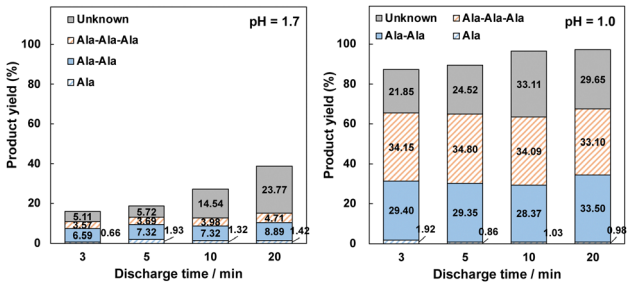


Fig. 2 Product yield *versus* discharge time with different initial pHs of 1.7 and 1.0. The initial pH of the sample solutions was adjusted to pH 1.7 and 1.0. [**Ala-DKP**] = 100 mM (10 mL), initial temperature: 25 °C, discharge frequency: 50 pps, and discharge time: 3–20 min.

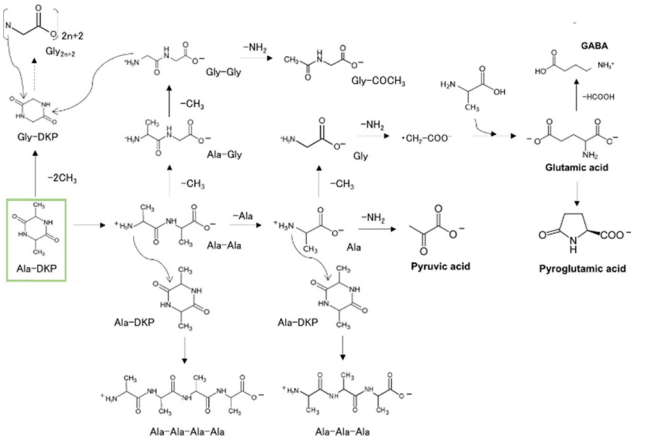


Scheme 1 Estimated reaction mechanism for the accumulation of higher oligopeptides.

Although **Ala-Ala-Ala-Ala-Ala** was not detected, the yield of **Ala-Ala-Ala** exceeded 30% at an initial pH of 1.0.

We monitored the reaction products at different discharge times of 3–20 min at pH 1.0–1.7, as shown in Fig. 2. The amount of **Ala-Ala** and **Ala-Ala-Ala** increased slightly with an increase in the discharge time from 3 to 20 min at pH 1.7. The yields of **Ala-Ala** and **Ala-Ala-Ala** were 8.89% and 4.71%, respectively, at pH 1.7. In addition, the number of unknown products increased with increasing discharge times up to 23.77% at pH 1.7. This indicates that the formation of **Ala-Ala** and **Ala-Ala-Ala** at pH 1.7 is faster than that of the unknown products. The number of oligopeptides gradually increased with increasing discharge times. This indicates that the formation of **Ala-Ala**, **Ala-Ala-Ala**, and unknown products proceeds quickly at the beginning of discharge compared to that at pH 1.7, where the extent of oligopeptides remained consistent at a discharge time of 3 min. The fact that both the yields of **Ala-Ala-Ala** and **Ala-Ala** reached approximately 30% and higher at pH 1.0 after a discharge time of 3-20 min was unexpected because **Ala-DKP** is considered a stable material. For a more detailed analysis of the reaction mechanism and behavior, we analyzed the reaction products discharged at an initial pH of 1.0 using LC-MS. The results are summarized in Table 2.

**Ala-Ala-Ala** and **Ala-Ala-Ala-Ala** were detected using LC-MS analysis. Also, different oligopeptides, including glycine, aspartic acid, glutamic acid residues and related peptides, were observed. **Gly-DKP**, **Ala-Gly**, and oligopeptides containing

Table 2 LC-MS analysis of the reaction products discharged at an initial pH of 1.0

| Compounds | Molecular formula | Formula mass/Da | Discharge time/min | | | |
|---|---|---|---|---|---|---|
| | | | 3 | 5 | 10 | 20 |
| **Ala-DKP** | $C_6H_{10}N_2O_2$ | 141.0664 | MP | MP | MP | MP |
| **Ala** | $C_3H_7NO_2$ | 88.0399 | +++ | +++ | +++ | +++ |
| **Ala-Ala** | $C_6H_{12}N_2O_3$ | 159.0770 | MP | MP | MP | MP |
| **Ala-Gly** | $C_5H_{10}N_2O_3$ | 145.0613 | ++ | ++ | ++ | ++ |
| **Ala-Pro** | $C_8H_{14}N_2O_3$ | 185.0926 | ++ | +++ | +++ | +++ |
| **Gly-DKP** | $C_4H_6N_2O_2$ | 113.0351 | ++ | ++ | ++ | +++ |
| **Ala-Ala-Ala** | $C_9H_{17}N_3O_4$ | 230.1141 | + | + | + | + |
| **Ala-Ala-Ala-Ala** | $C_{12}H_{22}N_4O_5$ | 301.1512 | ND | + | + | ++ |
| **Gly** | $C_2H_5NO_2$ | 74.0242 | ND | ND | ND | + |
| **Gly-Gly** | $C_4H_8N_2O_3$ | 131.0457 | ND | +++ | +++ | ++ |
| **Gly-Gly-Gly** | $C_6H_{11}N_3O_4$ | 188.0671 | + | + | ++ | ++ |
| **Gly-Gly-Gly-Gly** | $C_8H_{14}N_4O_5$ | 245.0886 | + | + | + | ++ |
| **Gly-Gly-Gly-Gly-Gly-Gly** | $C_{12}H_{20}N_6O_7$ | 359.1315 | ++ | ++ | ++ | + |
| **Gly-COCH$_3$** | $C_4H_7NO_3$ | 116.0348 | ++ | ++ | +++ | +++ |
| **Gly-Phe** | $C_{11}H_{14}N_2O_3$ | 222.1005 | + | + | ++ | ++ |
| **Asp** | $C_4H_7NO_4$ | 132.0297 | + | + | ND | + |
| **Asp-Asp** | $C_8H_{12}N_2O_7$ | 247.0566 | + | + | ND | ++ |
| **Asp-Asp-Asp** | $C_{12}H_{17}N_3O_{10}$ | 247.0566 | ND | ND | + | + |
| **Glu** | $C_5H_9NO_4$ | 146.0453 | + | ++ | ++ | ++ |
| **Glu-Glu** | $C_{10}H_{16}N_2O_7$ | 275.0879 | + | ND | ++ | ++ |
| **Glu-Glu-Glu** | $C_{15}H_{23}N_3O_{10}$ | 404.1305 | ND | ++ | ++ | ++ |
| **Glu-Glu-Glu-Glu** | $C_{20}H_{30}N_4O_{13}$ | 534.1810 | ++ | ++ | ++ | ++ |
| Pyruvic acid | $C_3H_4O_3$ | 87.0082 | — | + | — | + |
| Acetic acid | $C_2H_4O_2$ | 59.0133 | ND | ND | ND | + |
| Pyroglutamic acid | $C_5H_7NO_3$ | 128.0348 | + | + | ++ | ++ |

Major peaks: MP, detected area >200: +++, detected area 20–200: ++, detected area <20: +, and not detected: NDInitial pH: 1.0, [**Ala-DKP**] = 100 mM (10 mL), initial temperature: 25 °C, discharge frequency: 50 pps, and discharge time: 3–20 min.

glycine residues up to the hexamers were detected using LC-MS. This suggests that oligopeptide elongation proceeds but that demethylation occurs during or after oligopeptide elongation from **Ala-DKP**. In addition, the detection of pyruvic acid and *N*-acetylglycine. (**Gly-COCH3**) indicated that deamination occurs during irradiation with the discharge plasma. Based on the products detected by GC, LC, and LC-MS, we proposed a chemical network pathway for the formation of higher oligopeptides with different amino acid residues from **Ala-DKP**, as shown in Scheme 1.

In our previous study, we demonstrated a possible scheme for the formation of **Ala-Ala-Ala** and **Ala-Ala-Ala-Ala** from an **Ala-DKP** solution that was initially prepared at pH 4.6. In this study, we identified oligopeptides containing glycine and glutamic acid residues that were not originally added to the reaction mixture. According to our previous estimation, **Ala-Ala** and **Ala** were formed from the discharge plasma from the **Ala-DKP** solution. This would also occur in the present system, as shown in Scheme 1, where higher alanine residue oligopeptides are formed from **Ala-Ala** and **Ala** by attacking **Ala-DKP**. The formation of **Ala** and **Ala-Ala** is preferential as compared with that at pH 1.7 leading to the higher yields of **Ala-Ala-Ala** and **Ala-Ala-Ala-Ala**. In contrast, we detected evidence of deamination and demethylation based on LC-MS. Thus, it is reasonable that **Gly-DKP**, **Ala-Gly**, and **Gly-Gly** were formed by the demethylation of **Ala-DKP** and **Ala-Ala**. Higher oligopeptides containing glycine residues, such as **Gly-Gly-Gly-Gly** and **Gly-Gly-Gly-Gly-Gly**, are presumably formed by the same mechanism that was proposed for oligopeptides containing alanine residues, such as **Ala-Ala-Ala-Ala**. However, it is assumed that pyruvic acid and *N*-acetylglycine are formed by the deamination of **Gly-Gly** and alanine. Trace amounts of oligopeptides containing glutamic acid were also detected. Glutamic acid is produced by the reaction of alanine with a radical formed from glycine by deamination. Pyroglutamic acid is probably formed by the dehydration of glutamic acid in local high-temperature environments owing to the discharge plasma. This theory is reasonable because the hydrothermal dehydration of glutamic acid is possible.[13] In addition, the elongation of glutamic acid proceeds *via* the same mechanism as that of oligopeptides containing alanine residues. This estimated reaction network was consistent with the reaction mechanism of **Ala-DKP** at pH 4.6. In addition, an extra pathway forming oligopeptides containing glycine and glutamic acid residues was involved at pH values of 1.0 and 1.7.

### Importance of oligopeptide formation from the viewpoint of chemical evolution on Hadean Earth

**Ala-DKP** is a stable and terminal product of the chemical synthesis of oligopeptides in both fundamental and practical applications. From the viewpoint of origin-of-life studies, the formation of oligopeptides is normally examined under neutral pH conditions. In addition, the use of DKP as a reactant for the formation of higher oligopeptides has rarely been investigated under simulated primitive Earth conditions.[26,27] Thus, the discovery of an efficient oligopeptide from DKP was impressive. In addition, it is assumed that the water and ocean were very acidic (approximately a pH of 1.0) on the early Hadean Earth.[28] Acidic conditions would have been present through the accumulation of volcanic gas emissions and thunder discharges, which is suggested by the present study. These conditions are generally considered unsuitable for the formation of higher oligopeptides. In addition, our study provides very suggestive findings regarding the possibility of chemical environments for the formation of oligopeptides under very acidic conditions using DKP. In addition, the reaction mechanism, which presumably includes the radical process, is not known to be a general process for oligopeptide formation. Although oligopeptides are thought to elongate by the consecutive dehydration of a single oligopeptide with a single amino acid,[11–13] this study shows an alternative elongation pathway of oligopeptides through radical intermediates. In addition, this study suggests the possibility of forming oligopeptides containing a variety of amino acid residues from DKP and oligopeptides by deamination and demethylation.

### Evaluation of the proposed oligopeptide formation as a green process

According to our previous study, an inspection of the current–voltage profile provides valuable information regarding the reaction mechanisms of thermal or nonthermal plasma. A detailed comparison of the current–voltage profiles was attempted between the samples initially prepared at pH values of 4.6 and 1.0. The current–voltage profiles for the sample initially prepared at pH values of 4.6 and 1.0 are shown in Fig. 3. Photographs of the discharge plasma at initial pH values of 4.6 and 1.0 are shown in Fig. 4. In general, the voltage profile of the samples at an initial pH of 4.6 showed a small maximum between 100 and 200 ns, and the current peak mirrors the

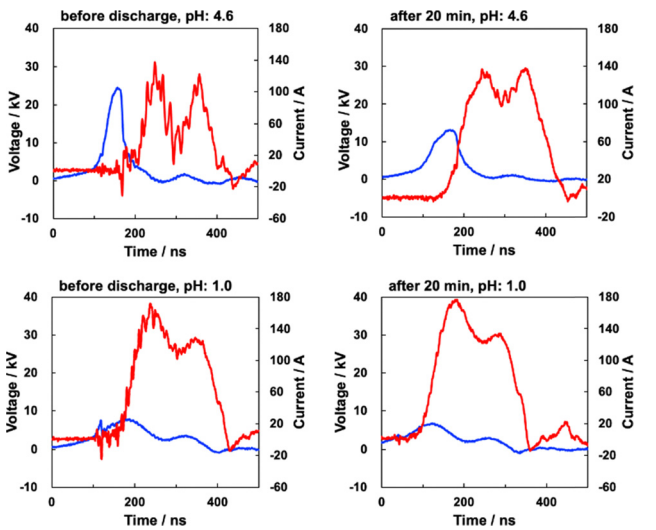


Fig. 3 Voltage (blue) and current (red) profiles by irradiation of the nano-pulsed discharge plasma. Irradiation time: left: before discharge and right: after 20 min irradiation of the nano-pulsed discharge plasma. Initial pH: top: 4.6; bottom: 1.0. [**Ala-DKP**] = 100 mM (10 mL), initial temperature: 25 °C, and discharge frequency: 50 pps.

 

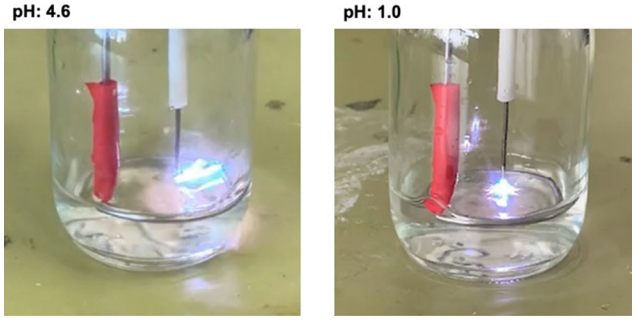


Fig. 4 Observation of lightning by the discharge plasma for samples at different initial pHs. Initial pH: left: 4.6 and right: 1.0, [**Ala-DKP**] = 100 mM (10 mL), initial temperature: 25 °C, discharge frequency: 50 pps, and discharge time: 20 min.

voltage peak during the first 100–200 ns after being irradiated with the nano-pulsed discharge. The voltage initially increased to approximately 25 kV before decreasing to approximately 15 kV after being irradiated with the nano-pulsed discharge plasma. The current remained constant with increasing irradiation times and two peaks were observed in the current profiles (Fig. 3). The synchronization of the rapid decrease and increase of the voltage and current, respectively, indicates an arc discharge plasma for the sample at an initial pH of 4.6 (Fig. 3). The maximum voltage in the time range of 100–200 nm and the maximum current at the first peak are visualized as functions of the discharge time in Fig. S3 (ESI†). The fact that the peak voltage decreased after 10–20 min of discharging indicates the occurrence of a dielectric breakdown by the repetitive irradiation of the nano-pulsed discharge plasma. This could be due to the increase in the acidity, temperature, and humidity in the reactor vessel, where steam may supply electrons.

However, the profiles of the solutions prepared initially at pH 1.0 are different from those initially prepared at pH 4.6. The current–voltage profiles at pH 1.0 reflect an arc discharge, where the voltage was considerably smaller and the current was greater than those at pH 4.6. The peak voltage at pH 1.0, which remained constant after 10–20 min of discharge irradiation, was significantly lower than that at the initial pH of 1.0. In addition, the magnitude of the current at an initial pH of 1.0 is greater than that at an initial pH of 4.6 and increased with increasing discharge times. At pH 1.0, the conductivity of the solution increases owing to the formation of nitric acid, which causes a dielectric breakdown.[29] At the same time, the current profile at pH 1.0 indicates that the current flows preferably to the aqueous phase rather than to the ground electrode.

The current–voltage profile for the sample at an initial pH of 4.6 is similar to that at an initial pH of 1.0. There is an approximate trend for the peak current–voltage profile for the sample at an initial pH of 4.6 as it becomes similar to that of the sample at an initial pH of 1.0 owing to a decrease in the pH due to the formation of nitric acid.

### Discharge energy balance estimation

The energy supplied by a single-pulse shot can be calculated as a function of the discharge time according to eqn (1), where $P$, $V$, $I$, and $E$ indicate the electric power, voltage, current, and energy, respectively. The relationship between the energy of a single pulse and the irradiation time is shown in Fig. S4 (ESI†).

$$P = V \times I \quad (1)$$

$$E = \int VI\,\mathrm{d}t \quad (2)$$

In general, the discharge energy supplied at pH 1.0 is much greater than that at pH 4.6. This is consistent with the assumption that a dielectric breakdown readily occurs at pH 4.6. The energy supplied by the discharge plasma for the sample at an initial pH of 4.6 increased with increasing irradiation times. The energies of a single-pulse shot at irradiation times of 0 and 20 min were 8.7 and 38.1 mJ, respectively. Although the peak voltage at 0 min was higher than that at 20 min, the current–voltage profile showed a less overlap of the current and voltage at 100–200 ns, indicating a low-energy supplement. In addition, the energy for a single-pulse shot was in the range 85–90 mJ for the samples with an initial pH of 1.0. The magnitude is greater than that for samples at an initial pH of 4.6 and the energy for samples at an initial pH of 4.6 becomes closer to that at pH 1.0 with increasing irradiation times. This suggests that the efficiency of the discharge plasma for samples at an initial pH of 1.0 is higher than that at pH 4.6, and the efficiency for samples at pH 4.6 increases with increasing irradiation times by the formation of nitrate.

The energy balance, which is converted into heat accumulated in an aqueous solution, can be estimated based on the magnitude of a single-pulse shot. The heat energy obtained from the aqueous solution (10 mL) was calculated to be 787 J. The estimated value of a single-pulse shot at an irradiation time of 10 min (21.2 mJ per shot) was approximately applied as an average value based on the straight line of the relationship between the energy of a single-pulse shot and the irradiation time (Fig. S4, ESI†). The total number of shots for 20 min of irradiation with 50 pps is 60 000 shots, so the energy supply from the nano-pulsed discharge is 1274 J. According to this calculation, at least 62% of the energy of a discharge plasma was used for heating the aqueous solution because the release of heat into the atmosphere was not considered. The estimation of the energy supplement efficiency for chemical processes is important.

## Conclusions

In this study, we identified an efficient pathway for oligopeptide formation using pulsed discharge plasma. The conversion of **Ala-DKP** to **Ala-Ala** and **Ala-Ala-Ala** at pH 1.0 exceeded 60%. This is very high compared to other environmentally friendly processes for the formation of oligopeptides,[11–13,30] where the formation of DKP is advantageous for the formation of oligopeptides and does not inhibit oligopeptide elongation.[31] From the viewpoint of chemical evolution on the Hadean Earth, this study demonstrated the importance of a continuous energy supply for the formation of biomolecules under prebiotic conditions. In addition, the fact that the experimental setup

using nano-pulsed discharge plasma is reproducible shows that this type of plasma discharge is a very useful experimental approach for both the fundamental and practical investigation of oligopeptides in aqueous solutions. This finding contrasts with the fact that the formation of DKP is regarded as a barrier to the elongation of higher oligopeptides. Furthermore, this process proceeded under highly acidic conditions. These findings would provide useful insights into the chemical evolution of oligopeptides and the development of environmentally friendly oligopeptide formation processes.

## Author contributions

Mitsuru Sasaki and Kunio Kawamura contributed to the management, leadership, and coordination of the research activity planning and execution, as well as the reviewing and editing of the original draft, specifically with the critical review, commentary, and revision. Kouki Nonaka and Yuka Sakai contributed to the research and investigation by specifically performing experiments and data collection. They also contributed to the preparation and writing of the original draft. Tetsuo Homma contributed to the product analysis by LC/MS. Tomohiro Furusato contributed to the development of the pulsed arc discharge equipment.

## Data availability

Details of the experiments are available within the article and the ESI.†

## Conflicts of interest

There are no conflicts to declare.

## Acknowledgements

This research was supported by the Collaborative Research Project of the Institute of Pulsed Power Science (IPPS) at Kumamoto University in 2010, the Institute of Industrial Nanomaterials (IINa) at Kumamoto University in 2020, and the International Research Organization for Advanced Science and Technology (IRAOST) at Kumamoto University in 2020. This research was financially supported by the MEXT Grant-in-Aid for Scientific Research (B) (grant number JP19H02017).

## Notes and references

1 A. A. Bahar and D. Ren, *Pharmaceuticals*, 2013, **6**, 1543–1575.
2 A. Sánchez and A. Vázquez, *Food Qual. Saf.*, 2017, **1**, 29–46.
3 E. D. Santis and M. D. Ryadnov, *Chem. Soc. Rev.*, 2015, **44**, 8288–8300.
4 J. Wang, K. Liu, R. Xing and X. Yan, *Chem. Soc. Rev.*, 2016, **45**, 5589–5604.
5 G. Liu, Q. T. Nguyen, E. Chow, T. Böcking, D. B. Hibbert and J. J. Gooding, *Electroanalysis*, 2006, **12**, 1141–1151.
6 N. P. Damayanti, K. Buno, S. L. V. Harbin and J. M. K. Irudayaraj, *ACS Sens.*, 2019, **4**, 562–565.
7 G. B. Fields and R. L. Noble, *Int. J. Pept. Protein Res.*, 1990, **35**, 161–214.
8 D. J. Gravert and K. D. Janda, *Chem. Rev.*, 1997, **97**, 489–509.
9 J. A. Baross and S. E. Hoffman, *Origins Life Evol. Biospheres*, 1985, **15**, 327–345.
10 N. G. Holm and E. M. Andersson, *Planet. Space Sci.*, 1995, **43**, 153–159.
11 E. Imai, H. Honda, K. Hatori, A. Brack and K. Matsuno, *Science*, 1999, **283**, 831–833.
12 K. Kawamura, T. Nishi and T. Sakiyama, *J. Am. Chem. Soc.*, 2005, **127**, 522–523.
13 K. Kawamura and M. Shimahashi, *Naturwissenschaften*, 2008, **95**, 449–454.
14 M. Y. A. Mollah, R. Schennach, J. Patscheider, S. Promreuk and D. L. Cocke, *J. Hazard. Mater.*, 2000, **79**, 301–320.
15 B. Jiang, J. Zheng, S. Qiu, M. Wu, Q. Zhang, Z. Yan and Q. Xue, *Chem. Eng. J.*, 2014, **236**, 348–368.
16 Y. Hayashi, N. Takada Wahyudiono, H. Kanda and M. Goto, *J. Supercrit. Fluids*, 2017, **120**, 403–407.
17 C. S. C. Issasi, K. Mori, R. M. Ibarra, M. Sasaki, A. T. Quitain, T. Kida, S. Okubayashi and T. Furusato, *ACS Appl. Polym. Mater.*, 2022, **4**, 74–83.
18 C. S. C. Issasi, R. M. Ibarra and M. Sasaki, *Nanocomposites*, 2022, **8**, 136–141.
19 T. Kiyan, M. Sasaki, T. Ihara, T. Namihira, M. Hara, M. Goto and H. Akiyama, *Plasma Processes Polym.*, 2009, **6**, 778–785.
20 B. R. Locke and K. Y. Shih, *Plasma Sources Sci. Technol.*, 2011, **20**, 034006.
21 M. Sasaki, Y. Miyagawa, K. Nonaka, R. Miyanomae, A. T. Quitain, T. Kida, M. Goto, T. Honma, T. Furusato and K. Kawamura, *Sci. Nat.*, 2022, **109**, 33.
22 W. L. Chameides, D. H. Stedman, R. R. Dickerson, D. W. Rusch and R. J. Cicerone, *J. At. Sci.*, 1977, **34**, 143–149.
23 Y. L. Yung and M. B. Mcelroy, *Science*, 1979, **203**, 1002–1004.
24 T. Namihira, S. Tsukamoto, D. Wang, S. Katsuki, R. Hackam, K. Okamoto and H. Akiyama, *IEEE Trans. Plasma Sci.*, 2000, **28**, 109–114.
25 S. Sakai, M. Matsuda, D. Wang, T. Namihira, H. Akiyama, K. Okamoto and K. Toda, *Acta Phys. Pol., A*, 2009, **115**, 1104–1106.
26 M. Nagayama, O. Takaoka, K. Inomata and Y. Yamagata, *Origins Life Evol. Biospheres*, 1990, **20**, 249–257.
27 S. Fuchida, H. Naraoka and H. Masuda, *Origins Life Evol. Biospheres*, 2017, **47**, 83–92.
28 S. Maruyama, M. Ikoma, H. Genda, K. Hirose, T. Yokoyama and M. Santosh, *Geosci. Front.*, 2013, **4**, 141–165.
29 H. Guo, H. Wang, Q. Wu and J. Li, *Sep. Purif. Technol.*, 2018, **190**, 288–296.
30 T. Munegumi, *Bull. Chem. Soc. Jpn.*, 2014, **87**, 1208–1215.
31 I. Coin, M. Beyermann and M. Bienert, *Nat. Protoc.*, 2007, **2**, 3247–3256.

 